ISSN 0023-1584, Kinetics and Catalysis, 2011, Vol. 52, No. 4, pp. 547–554. © Pleiades Publishing, Ltd., 2011.
Original Russian Text © Yu.I. Bauman, I.V. Mishakov, R.A. Buyanov, A.A. Vedyagin, A.M. Volodin, 2011, published in Kinetika i Kataliz, 2011, Vol. 52, No. 4, pp. 557–564.

Catalytic Properties of Massive Iron-Subgroup Metals in Dichloroethane Decomposition into Carbon Products

Yu. I. Bauman, I. V. Mishakov, R. A. Buyanov, A. A. Vedyagin, and A. M. Volodin

Boreskov Institute of Catalysis, Siberian Branch, Russian Academy of Sciences, Novosibirsk, 630090 Russia

e-mail: bauman@catalysis.ru

Received June 22, 2010

Abstract—The formation of nanocarbon materials on massive nickel, nichrome, and some other alloys via the carbide cycle mechanism is reported using 1,2-dichloroethane decomposition as an example. The role of the physical stage of the carbide cycle is elucidated, and massive metal surface activation methods ensuring the realization of this stage are considered. The surface layer of massive nickel or some nickel alloys is most effectively activated by the action of chlorine resulting from the catalytic decomposition of 1,2-dichloroethane. It has been demonstrated by ferromagnetic resonance (FMR) spectroscopy that the activation of the massive metal surface in 1,2-dichloroethane decomposition to nanocarbon is due to the surface undergoing crystal chemical restructuring. The microstructuring of the surface yields fine Ni particles similar in size (0.2–0.3 μm) and shape, whose FMR spectra are anisotropic and have similar magnetic resonance parameters. Both chlorine-free and chlorinated hydrocarbons decompose over these particles via the carbide cycle mechanism. It is demonstrated that it is possible to design catalytic reactors packed with massive nickel or its alloy. The nanocarbon material obtained in such a reactor will not be contaminated by components of conventional catalyst supports (Al, Mg, etc.). The stable performance temperature of the catalyst will be increased, and this will allow the equilibrium outlet methane concentration to be reduced.

DOI: 10.1134/S002315841104001X

The problem of finding catalytic systems for obtaining a wide variety of nanocarbons by hydrocarbon decomposition is of practical and scientific importance [1]. The numerous publications on this subject deal with various catalytic compositions possessing some useful properties for particular applications. The active components of these systems are fine particles of iron-subgroup metals or their alloys with other metals.

A wide variety of such systems are prepared by conventional coprecipitation or deposition of active components onto a support. In both cases, the heat-resistant support preventing the disperse phase of the catalyst from sintering is usually aluminum or magnesium oxide. Here, we consider the specific features and realization conditions of the so-called carbide cycle mechanism in 1,2-dichloroethane decomposition over massive nickel, nichrome, and some other alloys.

THEORY

The mechanism of the catalytic formation of nanocarbons has been investigated in detail [2–4]. It is referred to as the carbide cycle mechanism and consists of the following two stages.

The first is the chemical stage, specifically, the catalytic decomposition of the hydrocarbon to carbon and hydrogen via surface carbide-like intermediates on certain faces of disperse particles of iron-subgroup metals, their compositions, or their alloys containing other metals. The faces showing more pronounced catalytic properties, on which hydrocarbon decomposition takes place, are called the "frontal" faces.

This is followed by the physical stage, specifically, the diffusion of carbon atoms through the metal particle bulk from the "frontal" face to the "rear" face, the nucleation of the graphite phase on this face, and the growth of nanocarbons with different crystallographic and morphological characteristics.

Figure 1 illustrates 1,2-dichloroethane decomposition on a nickel particle. It is shown how the faces are situated and how carbon atoms diffuse from the "frontal" face to the "rear" face. It was established earlier that the functioning of the carbide cycle mechanism on disperse metal particles, which yields carbon nanostructures, is limited to the particle size range from 3 to 1000 nm [2], depending on the particle composition. This is due to the specific features of the diffusion transport of carbon atoms from the "frontal" face to the "rear" face of the metal particle and the formation of the carbon phase there. The smooth surfaces of massive metals do not have structural elements capable of functioning as the "rear" face. The metal particle faces on which the formation of nanocarbons takes place are meant here [4]. The carbon resulting from the chemical stage forms a thin coating on

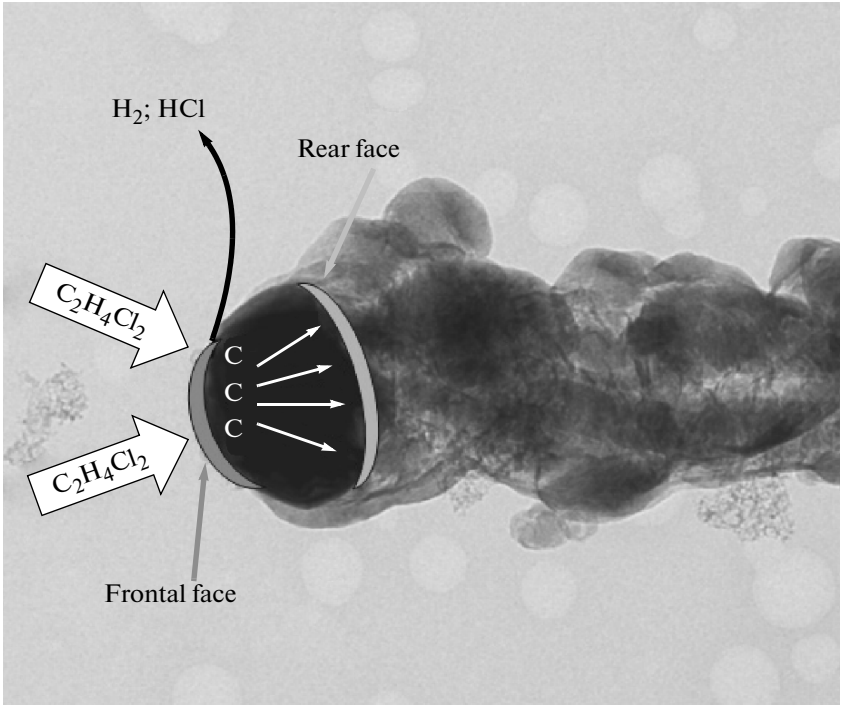

Fig. 1. 1,2-Dichloroethane decomposition on Ni/Al_2O_3 at 550°C.

the catalyst surface, thus insulating it from the gas phase, and the process dies down.

Thus, the key prerequisite for massive metals being usable in nanocarbon synthesis is that their surface has structures capable of functioning as the "rear" face. The size and topographic characteristics of these structures should be suitable for the physical stage of the process, which includes the diffusion transport of carbon atoms and the formation of a graphite-like phase. For the process to occur stably, the surface structure should either be resistant to destruction and deactivation or be reproduced during carbon formation (e.g., by metal surface erosion).

The concept of the carbide cycle mechanism applied to the surface of massive metals brings up the following questions:

What topography and structure should the massive metal surface have for both carbide cycle stages to take place on this surface and continue for a long time without deactivation? How should the surface layer of the metal be restructured (activated) to make it suitable for the physical stage?

What reaction conditions and metal surface properties are favorable for the so-called "root" growth of nanocarbons, in which metal particles do not separate from the surface of the massive metal, and what ones are favorable for crossover to so-called "head" growth, in which the separation of metal particles does take place?

What is the correlation between the morphology of the resulting nanocarbon and the surface (topographic, structural) properties of the massive metal on which it forms?

What advantages can be gained by combining the catalytic and structural functions in the design of a new type of catalytic reactor and in the implementation of the nanocarbon synthesis technology?

Clarification of these issues primarily needs search for methods of activation of the surface of massive metals and determination of the reaction conditions ensuring the stable run of both carbide cycle stages in nanocarbon formation.

EXPERIMENTAL

The massive metal catalysts were 0.1-mm-thick nickel ribbon (99.8% Ni, ~0.1% Fe, ~0.1% Co) and nichrome wire 0.1 mm in diameter (Kh20N80 brand, ~23% Cr, ~0.5% Fe, Ni to balance). To assess the generality of the experimental data, we additionally tested samples of chromel (90% Ni, ~10% Cr, ~0.3% Fe) and alumel (~94% Ni, ~0.5% Fe, ~2% Al, ~1% Si, ~2% Mn). The following chemicals were also used in our experiments: high-purity argon, hydrogen, and ethane; dried air; 1,2-dichloroethane (reagent grade); and concentrated HCl and HNO_3.

The surface of massive metals was activated in three ways: (1) etching with a mixture of concentrated HCl and

HNO_3 (3 : 1) for 3 min, (2) oxidative and reductive treatment at 550°C by alternating the oxidation of the sample in air with the reduction of the sample with hydrogen (redox treatment), and (3) treatment with hydrogen chloride resulting from the decomposition of chlorinated hydrocarbons.

Let us consider the third activation method in greater detail. We demonstrated earlier [5] that the decomposition of chlorinated hydrocarbons over nickel catalysts via the carbide cycle mechanism includes the following basic reactions:

$$3n\mathrm{Ni} + \mathrm{C}_n\mathrm{H}_m\mathrm{Cl}_k \longrightarrow n[\mathrm{Ni}_3\mathrm{C}] + k\mathrm{Cl} + m\mathrm{H}, \quad \text{(I)}$$

$$[\mathrm{Ni}_3\mathrm{C}] \longrightarrow 3\mathrm{Ni} + \mathrm{C},$$

$$\mathrm{Ni} + 2\mathrm{Cl} \longrightarrow \mathrm{NiCl}_2, \quad \text{(II)}$$

$$\mathrm{NiCl}_2 + 2\mathrm{H}(\mathrm{H}_2) \longrightarrow \mathrm{Ni} + 2\mathrm{HCl}, \quad \text{(III)}$$

$$\mathrm{H} + \mathrm{Cl} \longrightarrow \mathrm{HCl}, \quad \text{(IV)}$$

$$\mathrm{C} + 4\mathrm{H}(\mathrm{H}_2) \longrightarrow \mathrm{CH}_4. \quad \text{(V)}$$

The combination of reactions (II) and (III) causes the erosion (chemical rupture) of the surface of massive nickel. This activation procedure can produce surface structures (including an area of the "rear" face) favorable for the physical stage of the carbide cycle.

Experiments were carried out in flow reactor fitted with a McBain balance [6]. This allowed the coking of the catalysts to be monitored as the variation of their weight.

All samples were held in flowing hydrogen after they were placed into the reactor and the reactor was brought to the preset temperature. Thereafter, argon saturated with 1,2-dichloroethane vapor in a saturator was fed into the reactor. The weight of the catalyst sample was 3.0 ± 0.1 mg. The changes in the sample weight were measured at 2-min intervals.

Ferromagnetic resonance (FMR) spectra were recorded on an ERS-221 3-cm EPR spectrometer at room temperature. A specific feature of FMR applied to metals strongly absorbing microwave radiation is that it is necessary to use very small samples. In our experiments, the samples (0.5–1.0 mg) were placed in a quartz tube.

The elemental composition of the catalysts before and after the reaction was determined by inductively coupled plasma atomic emission spectroscopy (ICP-AES).

The morphology and structure of nanocarbons were studied by scanning electron microscopy (SEM) and transmission electron microscopy (TEM).

RESULTS AND DISCUSSION

Figure 2 shows SEM images of the surface of a nickel ribbon (Figs. 2a–2c) and nichrome wire (Fig. 2d). The surface of the untreated Ni ribbon (Fig. 2a) is smooth and does not contain structures suitable for the physical stage of nanocarbon formation. The acidic treatment (Fig. 2b) of the surface yields etch patterns, which form because of the crystal dissolution rate depending on the crystallographic direction. The resulting folded relief, which reveals different crystallographic faces, can contain areas suitable for the physical stage of the carbide cycle.

The redox treatment (Fig. 2c) loosens the surface to a greater extent and leads to more uniform surface structuring. The surface formed in this way is the most favorable for both stages of the carbide cycle.

The acidic treatment of the nichrome wire produces deep cavities in its surface layer. This can be explained by the preferential dissolution of iron and nickel. The wire surface subjected to redox treatment acquires roughness like that shown in Fig. 2c, but with a finer structure. Similar results were obtained for chromel and alumel.

These data suggest that the optimum method of activation of the massive metal surface for its restructuring is redox treatment. Acid etching is appropriate only for individual metals, because, as an alloy is etched, the difference between the dissolution rates of the constituent metals causes changes in the component ratio in the alloy and, accordingly, in the composition of the massive catalyst.

Next, we studied how the hydrocarbon decomposition rate and, accordingly, the nanocarbon formation rate depend on the method of activation of the massive metal. Ethane was chosen to be the model hydrocarbon. Experiments demonstrated that the surface of the metals subjected to acid etching or redox treatment does not initiate the carbide cycle mechanism. The surface gets covered with several carbon layers and hydrocarbon decomposition slows down. Therefore, these activation methods do not yield surface structures suitable for the physical stage of the carbide cycle.

Against the background of these facts, it is of particular interest to consider the decomposition of the chlorinated hydrocarbon 1,2-dichloroethane on massive metals. A specific feature of this reaction is that, at a certain chlorine-to-hydrogen ratio, nickel chlorination can occur on the catalyst surface to deactivate the catalyst completely. This catalyst deactivation can be prevented by introducing excess hydrogen into the reaction mixture. As is demonstrated in Fig. 3, the nickel catalyst is inactive in the absence of hydrogen and is fairly active in excess hydrogen. For this reason, the subsequent 1,2-dichloroethane decomposition experiments were carried out with reaction mixtures diluted with hydrogen to a hydrogen concentration of 37.5 vol %.

The first and second surface activation methods applied to the nickel ribbon produce only a weak effect, while the nichrome surface becomes significantly more active upon reconstruction (table). Nanocarbon formation on the untreated nichrome surface is observed only 3 h after the surface is brought into contact with the reaction mixture. The strongest activating effect on nichrome is exerted by the redox treatment because a uniform

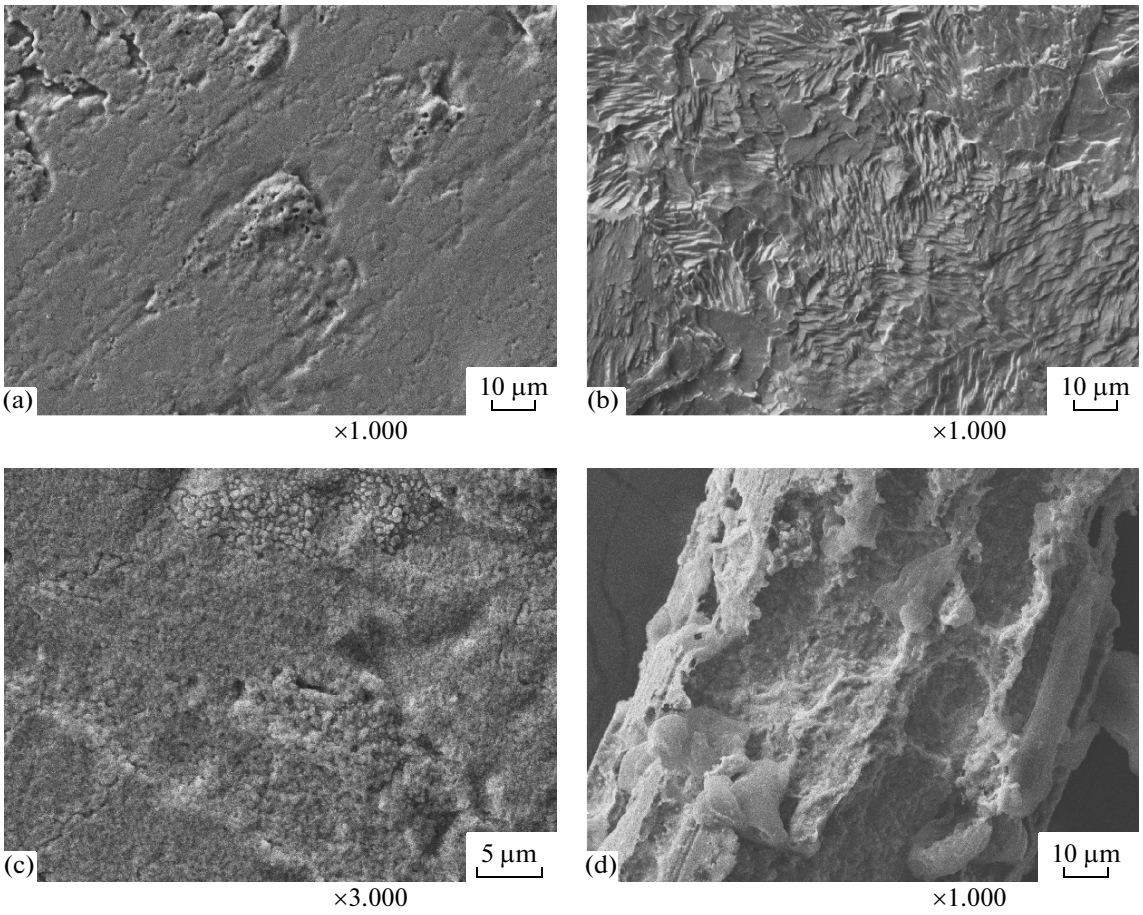

Fig. 2. SEM images of the (a–c) nickel ribbon and (d) nichrome wire surfaces: (a)untreated surface, (b, d) acid-etched surface, and (c) surface subjected to oxidative and reductive treatment.

microstructure of the surface is attained in this case. Thus, the pretreatment of the alloys produces more favorable conditions for subsequent surface loosening under the action of the H_2/HCl couple, shortening the induction period of the reaction.

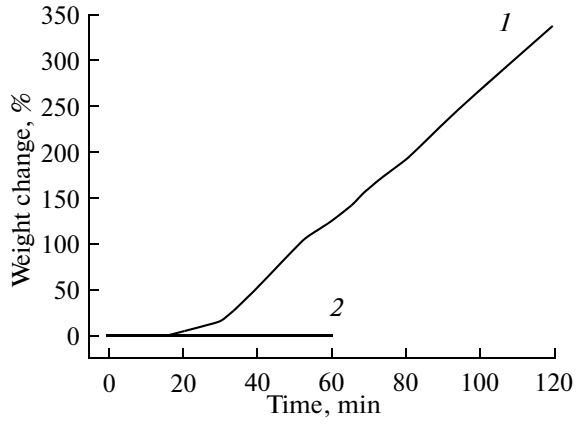

Fig. 3. Effect of excess hydrogen in the reaction mixture on the rate of 1,2-dichloroethane decomposition and nanocarbon formation on the nickel ribbon at 550°C: (*1*) excess hydrogen (37.5 vol %); (*2*) no hydrogen.

Further evidence of the activating effect of the redox mixture of H_2 and HCl is provided by the fact that the metal surface reconstructed under the action of released chlorine atoms is active in the decomposition of chlorine-free hydrocarbons.

As is demonstrated in Fig. 4 (curve *1*), 1,2-dichloroethane decomposition to nanocarbon on the nichrome wire at 600°C is accompanied by the erosion of the massive metal, which eventually causes its total disintegration. However, 1,2-dichloroethane decomposition does not terminate at this point, continuing on the resulting fine particles of nickel without any appreciable decrease in the reaction rate. This is evidence that, from the very beginning of the process, 1,2-dichloroethane decomposition in this system takes place on the resulting fine nickel particles having both "frontal" and "rear" areas necessary for the carbide cycle mechanism. It was hypothesized that these nickel particles would be active in the decomposition of ordinary hydrocarbons containing no chlorine. After 1,2-dichloroethane was replaced with

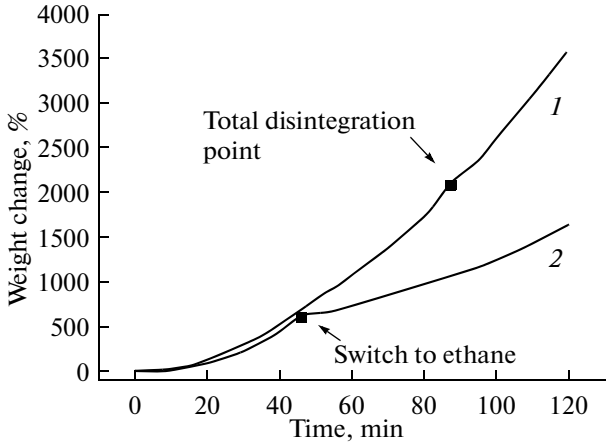

Fig. 4. Kinetics of nanocarbon formation on the nichrome wire at 600°C (*1*) in 1,2-dichloroethane decomposition and (*2*) after the replacement of 1,2-dichloroethane with ethane.

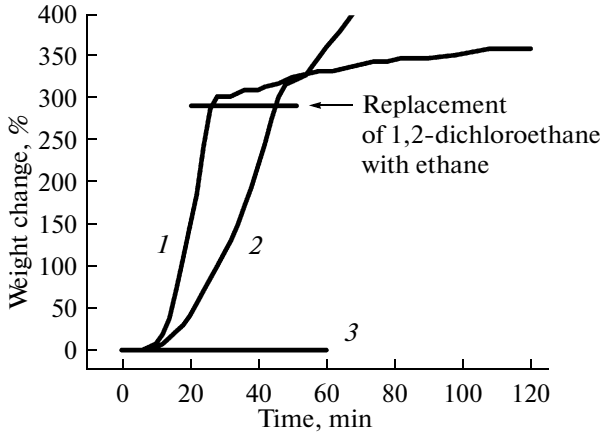

Fig. 5. Kinetics of nanocarbon formation on the nichrome wire at a hydrogen concentration of ~40 vol %: (*1*) replacement of 1,2-dichloroethane vapor with ethane at 700°C, (*2*) replacement of 1,2-dichloroethane vapor with ethane at 600°C, and (*3*) ethane decomposition at 700°C.

ethane (Fig. 4, curve *2*), the latter indeed decomposed on the fine nickel particles, although there was no further disintegration of the massive metal.

The initial portions of curves *1* and *2* in Fig. 5 characterize the nanocarbon formation rate in 1,2-dichloroethane decomposition on the nichrome wire. The inflection points in these curves indicate the switch from 1,2-dichloroethane vapor to ethane. Without being additionally activated with HCl, this catalyst is inactive in ethane decomposition (straight line *3*). These results provide further evidence that activation with the H_2 + HCl mixture makes the catalyst active in the decomposition of chlorine-free hydrocarbons (e.g., ethane) as well. Thus, in order to make the massive iron-subgroup metals promising hydrocarbon decomposition catalysts, it is necessary to ensure their self-disintegration during the reaction.

Earlier, we described the specific features of the formation of feathery carbon nanostructures [5, 6]. It might be expected that these features would show themselves in the reaction carried out on the massive metals. Figures 6a and 6b display the micrographs of the nanocarbons obtained by 1,2-dichloroethane decomposition at 550°C on the nichrome wire. These products appear as a bundle consisting of interlaced fragments of feathery carbon structures.

Of special interest is information concerning the metal surface structure, which largely determines the crystallographic and morphological properties of the resulting nanocarbon. Figures 6c and 6d show the micrographs of nanosized carbon bundles resulting from 1,2-dichloroethane decomposition at 550°C on the nickel ribbon pretreated by acid etching. It can be seen that the carbon filaments grow unidirectionally as an organized bundle reflecting the polycrystalline monodisperse structure of the nickel surface on which they form. This situation is not observed when carbon filaments grow on separate, unbound metal particles differing in size. Note that the ends of these filaments have no metal particles serving as filament growth generators in the "head" variant of the carbide cycle mechanism. Therefore, at least part of the carbon phase forms via the "root" variant of this mechanism; that is, the activated metal surface has "rear" areas necessary for nanocarbon growth.

However, in 1,2-dichloroethane decomposition both on the nickel ribbon and on the nichrome, alumel, and chromel wires, the major part of the nanocarbon consists of feathery structures as bundles containing included 0.15- to 0.3-μm metal particles. This is evidence of the "head" variant of the carbide cycle mechanism taking place. This brings up the natural question of what the ele-

Effect of the alloy treatment method on the induction period nanocarbon growth

Activation method	Induction period of nanocarbon growth, min	
	nickel ribbon	nichrome
No treatment	25	180
Acidic treatment	20	40
Redox activation	15	20

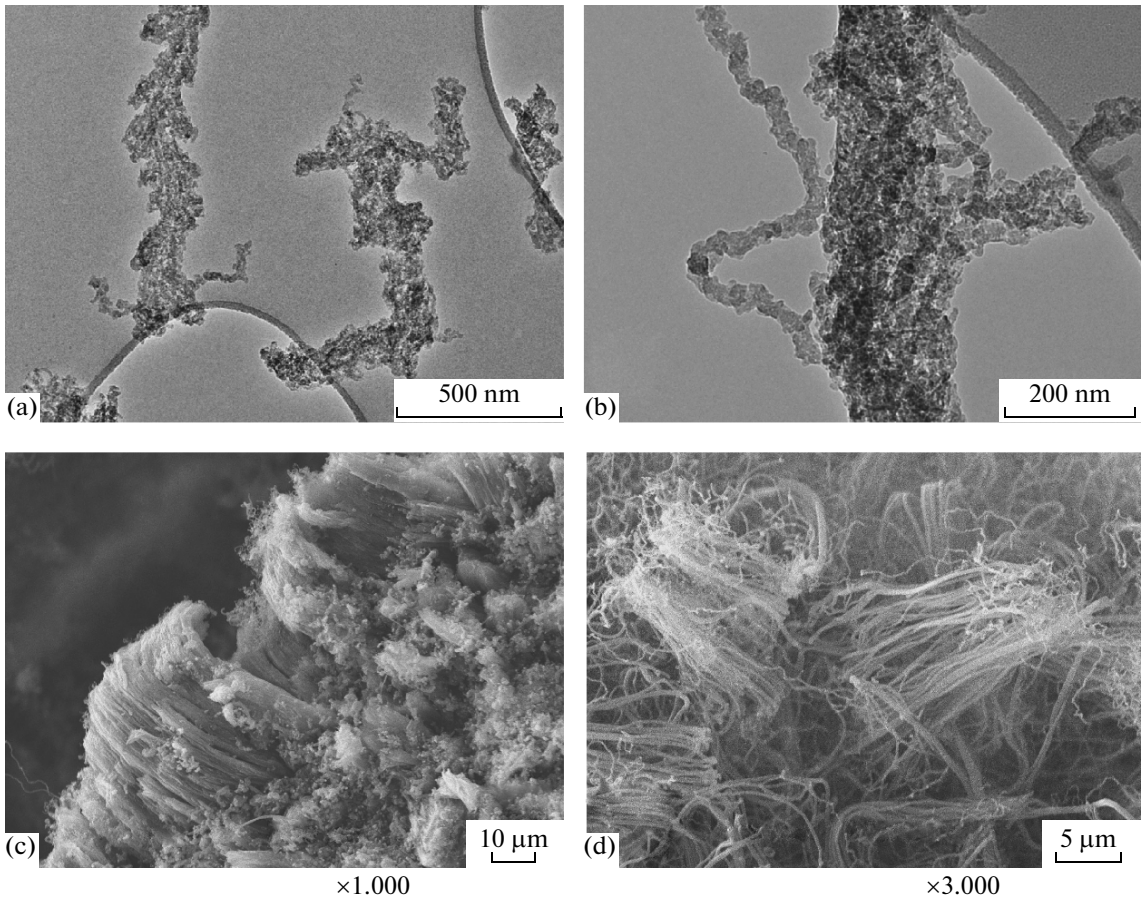

Fig. 6. Micrographs of the nanocarbon material obtained by 1,2-dichloroethane decomposition at (a, b, d) 550 and (c) 750°C on the (a, b) nichrome wire (TEM) and (c, d) nickel ribbon (SEM).

mental composition of these metal particles is and why their sizes vary within such a narrow range. These issues are of particular importance because the four samples examined differ in nature and composition.

In order to clarify these issues, we examined the above metals by FMR spectroscopy before and after their coking in 1,2-dichloroethane decomposition to nanocarbon.

The FMR method turned out to be very informative in this study. The screening of the four different materials (Fig. 7a) demonstrated that the initial, noncoked nickel and alumel samples give low-informative anisotropic FMR signals characteristic of large particles of a ferromagnetic metal [7]. This provided good reason to expect that any disintegration of these particles and a change in their morphology would alter their FMR spectrum. The coking of the nickel-containing alloys (Fig. 7b, curves *1*–*4*) and nickel metal (Fig. 7b, curves *5*) indeed led to similar FMR spectra for all samples due to the formation of fine nickel particles.

Note that nichrome, which contains up to 75% Ni, give no FMR signal at all (Fig. 7a, curve *1*). The signal from chromel (<90% Ni) is weak and is typical of fine nickel particles. It is therefore, expected that even the appearance of a small amount of fine nickel metal particles in these alloys will be noticeable well.

After the coking of the above four materials, we observed signals nearly identical in shape (*g*-factor, band width) for all samples (Fig. 7b). This is evidence of the formation of nickel metal particles identical in size and geometry. This effect is most pronounced for nichrome, which originally does not give any FMR spectrum. Therefore, coking causes a crystal chemical restructuring, producing fine nickel particles from the initial massive metal or alloy.

In the HRTEM images of the coked nichrome samples, we distinguished areas of feathery carbon bundles and metal inclusions. The carbon areas contained ~99.1 at % C and 0.9 at % Cl. The metal areas contained 92–96 at % Ni, 3.5–3.9 at % Fe, 0.2–0.6 at % Cr, and 1.1–4.3 at % Cl. As was mentioned above, the sizes of these particles are similar for the systems examined. Therefore, the catalyst undergoes structural and chemical self-organization in the decomposition of chlorinated hydrocarbons to nanocarbon via the carbide cycle mechanism.

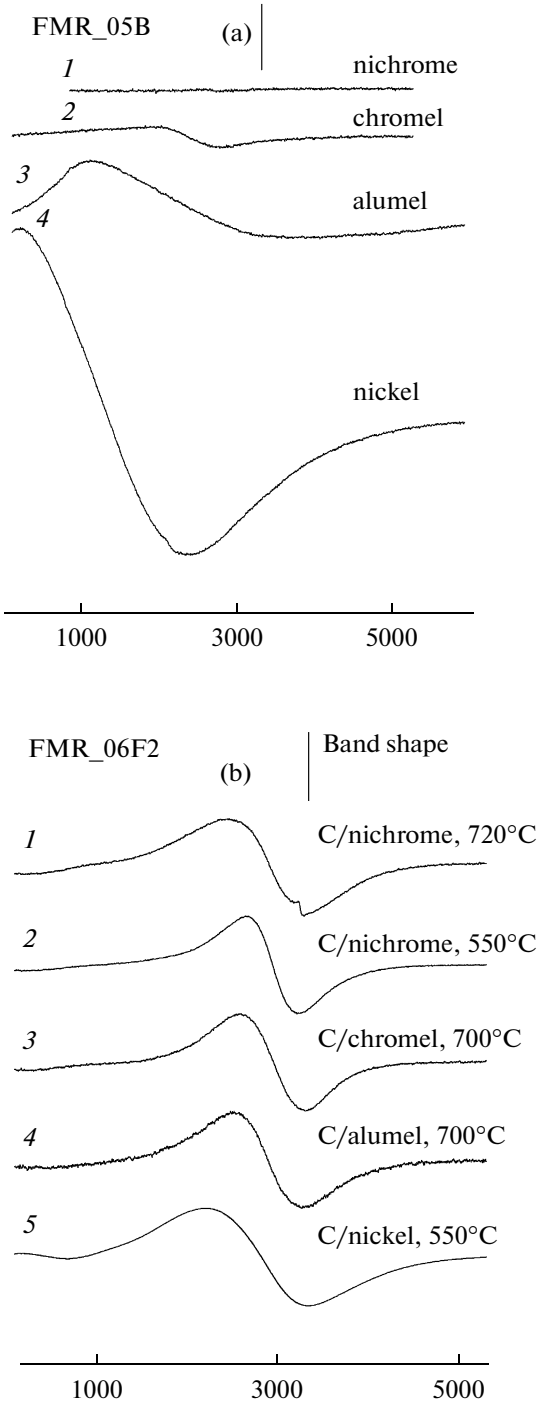

Fig. 7. (a) FMR spectra of massive samples of (*1*) nichrome, (*2*) chromel, (*3*) alumel, and (*4*) nickel before they were brought into contact with the reaction mixture (1,2-dichloroethane + H_2). (b) FMR spectra of the same samples coked at 550, 700, or 720°C.

The results of this study suggest that the iron-subgroup metals are promising as nanocarbon synthesis catalysts. A catalyst packing made from a massive metal will offer at least the following two advantages: it will contain no idle elements of conventional catalyst supports (Al, Si, Mg, etc.), and its thermal stability will make it possible to raise the reaction temperature and thus reduce the equilibrium concentration of methane resulting from reaction (V) in the gas leaving the reactor.

In prospect, the new catalysts based on massive metals and their alloys are expected to enable one to design a dual-purpose process combining nanocarbon produc-

tion and utilization of multicomponent chorine-containing waste.

ACKNOWLEDGMENTS

This work was carried out in the framework of the research program of the Kataliz Science and Education Center and was supported by the Ministry of Science and Education of the Russian Federation and by the Davison of Chemistry and Materials Science of the Russian Academy of Sciences (project no. 522).

REFERENCES

1. Rakov, E.G., *Usp. Khim.*, 2000, vol. 69, no. 1, p. 41.
2. Buyanov, R.A. and Chesnokov, V.V., *Khim. Interes. Ust. Razv.*, 1995, vol. 3, p. 177.
3. Chesnokov, V.V. and Buyanov, R.A., *Usp. Khim.*, 2000, no. 7, p. 675.
4. Buyanov, R.A. and Chesnokov, V.V., *Katal. Prom–sti.*, 2006, no. 2, p. 3.
5. Mishakov, I.V., Buyanov, R.A., Zaikovskii, V.I., Strel'tsov, L.A., and Vedyagin, A.A., *Kinet. Catal.*, 2008,vol. 49, no. 6, p. 868.
6. Mishakov, I.V., Chesnokov, V.V., Buyanov, R.A., and Pakhomov, N.A., *Kinet. Catal.*, 2001,vol. 42, no. 4, p. 543.
7. Slinkin, A.A., *Usp. Khim.*, 1968, vol. 37, no. 8, p. 1521.